Electronic Supporting Information

Silver(I) Nanoclusters of Carbazole-1,8-Bis(acetylide): from Visible to Near-infrared Emission

Xu Zhang,* Jin-Yun Wang, Ya-Zi Huang, Ming Yang, Zhong-Ning Chen*

State Key Laboratory of Structural Chemistry, Fujian Institute of Research on the Structure of Matter, Chinese Academy of Sciences, Fuzhou, Fujian 350002, China. E-mail: zhangxu@fjirsm.ac.cn, czn@fjirsm.ac.cn; University of Chinese Academy of Sciences Beijing, 100039, China

Experimental Section

General Procedures and Materials. All manipulations were conducted under a dry argon atmosphere using Schlenk techniques and vacuum-line systems unless otherwise specified. The solvents were dried, distilled, and degassed prior to use except that those for spectroscopic measurements were of spectroscopic grade. 2,6-Bis(diphenylphosphino)pyridine (dpppy)[1] and 3,6-di-*tert*-butyl-1,8-diethynyl-9H-carbazole (H_3decz)[2] were prepared by the literature procedures. Other reagents were purchased from commercial sources and used as received unless stated otherwise.

$[Ag_2(Hdecz)]_n$ (1a). To an aqueous (20 mL) solution of $AgNO_3$ (339.7 mg, 0.2 mmol) was added dropwise concentrated aqueous ammonia under vigorous stirring. When the suspended solution became clear, the addition of ammonia water was stopped. To this fresh prepared silver nitrate ammonia solution was added dropwise 1,4-dioxane (10 mL) solution of H_3decz (327.5 mg, 0.1 mmol). Upon stirring for 1d, red precipitate was fitrated and washed by water and then ethanol. After dried in vacuum, deep red product was quantitatively obtained. ICP analysis: Ag, 38.12 (calcd 39.86).

$[Ag_3(decz)]_n$ (1b). This polymer was prepared by the same synthetic procedure as that of $[Ag_2(Hdecz)]_n$ except using 3 equivalent $AgNO_3$ instead of 2. Upon dried in vacuum, dark red product was quantitatively obtained. ICP analysis: Ag, 48.39 (calcd 49.94).

$[Ag_8(dpppy)_4(decz)_2](ClO_4)_2$ (2). To a CH_2Cl_2 (15 mL) solution of dpppy (44.7 mg, 0.1 mmol) was added $[Ag_3(decz)]_n$ (32.4 mg) and $Ag(tht)ClO_4$ (14.8 mg, 0.05 mmol) with stirring for 12 h. The resulting yellow solution was separated to several test tubes and diethyl ether was layered onto the top of tubes. One week later, the product was isolated as yellow crystals. Yield: 62%. Anal. Calcd for $C_{164}H_{136}Ag_8Cl_2N_6O_8P_8$: C, 56.27; H, 3.92; N, 2.40. Found: C, 55.95; H, 4.01; N, 2.31. HRMS *m/z* (%): 1650.5574 (100) $[M–2ClO_4]^{2+}$ (calcd 1650.5568). ^{1}H NMR (400 MHz, CD_2Cl_2, ppm): 7.68-7.57 (m, 24H), 7.46-7.35 (m, 24H), 7.34-7.26 (m, 20H), 7.02 (t, 16H, J = 7.6 Hz), 6.54 (d, 4H, J = 1.6 Hz), 6.29 (t, 4H, J = 7.8 Hz), 5.48 (d, 8H, J = 7.8 Hz), 0.91 (s, 36H). ^{31}P NMR (162 MHz, CD_2Cl_2, ppm): 5.43 (dd, 8P, $J_{P\text{-}P}$ = 28 Hz, $J_{Ag\text{-}P}$ = 394 Hz). IR (KBr, cm^{-1}): 1986 (m, C≡C), 1096 (s, ClO_4).

$[Ag_{16}(dpppy)_4(Hdecz)_4(decz)_2](ClO_4)_2$ (3). To a CH_2Cl_2 (20 mL) solution of dpppy (44.7 mg, 0.1 mmol) was added $[Ag_3(decz)]_n$ (16.2 mg), $[Ag_2(Hdecz)]_n$ (54.1 mg) and $Ag(tht)ClO_4$ (14.8 mg, 0.05 mmol) with stirring for 12 h. The resulting dark red solution was separated to several test tubes and n-hexane was layered onto the top of tubes. One week later, the product was obtained as red crystals. Yield: 37%. Anal. Calcd for $C_{260}H_{228}Ag_{16}Cl_2N_{10}O_8P_8$: C, 55.12; H, 4.06; N, 2.47. Found: C, 55.01; H, 4.24; N, 2.33. HRMS *m/z* (%): 2733.0460 (100) $[M–2ClO_4]^{2+}$ (calcd 2733.0432). ^{1}H NMR (400 MHz, CD_2Cl_2, ppm): 10.07 (s, 2H), 9.31 (s, 2H), 8.14-8.06 (m, 4H), 7.99 (s, 2H), 7.95 (s, 2H), 7.90-7.71 (m, 12H), 7.68-7.57 (m, 12H), 7.54-7.33 (m, 22H), 7.26 (dd, 4H, J = 12.0 Hz, J = 7.5 Hz), 7.19 (t, 2H, J = 7.1 Hz), 7.12 (d, 2H, J = 8.0 Hz), 7.03 (t, 2H, J = 7.4 Hz), 6.98-6.83 (m, 12H), 6.76-6.68 (m, 6H), 6.64 (d, 2H, J = 1.6 Hz), 6.55 (d, 2H, J = 1.7 Hz), 6.53-6.41 (m, 8H), 6.36 (d, 2H, J = 1.6 Hz), 6.33-6.19 (m, 6H), 6.04-5.91 (m, 6H), 5.83 (t, 4H J = 8.1 Hz), 5.76 (d, 2H, J = 1.6 Hz), 5.54 (t, 2H, J = 7.4 Hz), 1.64 (s, 18H), 1.15 (s, 36H), 0.96 (s, 18H), 0.57 (s, 18H), 0.19 (s, 18H). ^{31}P NMR (162 MHz, CD_2Cl_2, ppm): 15.53 (dd, 2P, $J_{P\text{-}P}$ = 41 Hz, $J_{Ag\text{-}P}$ = 578 Hz), 9.56-7.44 (m, 3P), 6.97 (d, 2P, $J_{Ag\text{-}P}$ = 450 Hz), 5.75-5.27 (m, 1P, overlaped), 4.98 (dd, 1.20P, $J_{P\text{-}P}$ = 30 Hz, $J_{Ag\text{-}P}$ = 412 Hz), 4.27 (dd, 0.80P, $J_{P\text{-}P}$ = 30 Hz, $J_{Ag\text{-}P}$ = 412 Hz). IR (KBr, cm^{-1}): 2002 (m, C≡C), 1096 (s, ClO_4).

$[Ag_{29}(dpppy)_6(Hdecz)_2(decz)_8](ClO_4)$ (4). To a CH_2Cl_2 (30 mL) solution of dpppy (53.7 mg, 0.12 mmol) was added $[Ag_3(decz)]_n$ (103.7 mg), $[Ag_2(Hdecz)]_n$ (21.6 mg) and $Ag(tht)ClO_4$ (7.4 mg, 0.025 mmol) with stirring for 12 h. The resulting dark red solution was separated to several test tubes and n-hexane was layered onto the top of tubes. One week later, the product was obtained as dark red crystals. Yield: 23%. Anal. Calcd for $C_{414}H_{360}Ag_{29}ClN_{16}O_4P_{12}$: C, 54.29; H, 3.96; N, 2.45. Found: C, 54.03; H, 3.99; N, 2.38. HRMS *m/z* (%): 4529.8938 (100) $[M–ClO_4+H]^{2+}$ (calcd 4529.9035), 4583.8432 $[M–ClO_4+Ag]^{2+}$ (calcd 4583.8521). ^{1}H NMR (400 MHz, CD_2Cl_2, ppm): 8.98 (s, 2H), 8.84 (d, 2H, J = 1.2 Hz), 8.11 (d, 4H, J = 1.6 Hz), 8.08-7.98 (m, 12H), 7.90 (dd, 6H, J = 5.1 Hz, J = 1.7 Hz), 7.89-7.79 (m, 12H), 7.74 (d, 4H, J = 1.8 Hz), 7.68-7.50 (m, 22H), 7.45 (s, 4H), 7.37 (t, 8H, J = 7.3 Hz), 7.33-7.12 (m, 32H), 7.09 (t, 8H, J = 7.4 Hz), 6.95 (d, 2H, J = 1.7 Hz), 6.92-6.85 (m, 6H), 6.83-6.71 (m, 8H), 6.71-6.54 (m, 8H), 6.51 (d, 2H J = 7.8 Hz), 6.30 (dd, 4H, J = 11.3 Hz, J = 7.5 Hz), 6.18 (t, 4H, J = 8.6 Hz),

6.15-5.97 (m, 14H), 5.90 (d, 2H, J = 1.6 Hz), 5.83 (d, 2H, J = 1.4Hz), 5.77 (d, 2H, J = 7.4 Hz), 5.58-5.47 (m, 4H), 5.46-5.38 (m, 6H), 1.61 (s, 18H), 1.46 (s, 18H), 1.35 (s, 18H), 1.22 (s, 18H), 1.07 (s, 18H), 1.06 (s, 18H), 0.73 (s, 18H), 0.50 (s, 18H), 0.42 (s, 18H), 0.16 (s, 18H). ^{31}P NMR (162 MHz, CD_2Cl_2, ppm): 10.35-9.28 (m, 1P), 8.44-4.99 (m, 6P), 4.08-2.38 (m, 3P), 1.04-0.33 (m, 2P). Owing to the low solubility of **4** and the overlap in the ^{31}P NMR spectrum, the Ag−P and P−P couplings could not be resolved unambiguously. IR (KBr, cm^{-1}): 1994 (m, C≡C), 1096 (s, ClO_4).

Physical Measurements. UV-Vis absorption spectra were measured on a Perkin-Elmer Lambda 35 UV-Vis spectrophotometer. Infrared spectra (IR) were recorded on a Bruker VERTEX 70 FT-IR spectrophotometer with KBr pellets. Elemental analysis (C, H, N) were carried out on a Perkin-Elmer model 240 C elemental analyzer. ICP analyses were performed on an Ultima2 Inductively Coupled Plasma OES spectrometer. High resolution mass spectrometry (HRMS) was performed on a Bruker Impact II Q-TOF mass spectrometer using dichloromethane and methanol mixtures as mobile phases. ^{1}H and ^{31}P NMR spectra were recorded on a Bruker Avance III 400 spectrometer with $SiMe_4$ and H_3PO_4 as internal and external references, respectively. Emission and excitation spectra were recorded on a Perkin-Elmer LS55 luminescence spectrometer with a red-sensitive photomultiplier type R928. Emission lifetimes in solid states and degassed solutions were determined on an Edinburgh analytical instrument (FLS920 fluorescence spectrometer). The absolute emission quantum yield (Φ_{em}) in degassed dichloromethane solution and solid states were determined by the integrating sphere (142 mm in diameter) using Edinburgh FLS920 Spectrofuorophotometer.

Crystal Structural Determination. Crystals suitable for X-ray crystallographic measurement were grown by layering n-hexane (ethyl ether for cluster **2**) onto CH_2Cl_2 solutions. Data collection of cluster **2** was performed on Mercury CCD diffractometer by the ω scan technique at room temperature using graphite-monochromated Mo-Ka (λ = 0.71073 A˚) radiation, and the CrystalClear software package was used for data reduction and empirical absorption correction. The data of complexes **3** and **4** were collected on Bruker diffractometer MD2 of BL17B beamline of National Center for Protein Sciences Shanghai (NCPSS) at Shanghai Synchrotron Radiation Facility, and the data were processed by using

the HKL3000 program. All the structures were solved by direct methods. The heavy atoms were located from E-map, and the rest of the non-hydrogen atoms were found in subsequent Fourier maps. All non-hydrogen atoms were refined anisotropically, while the hydrogen atoms were generated geometrically and refined with isotropic thermal parameters. The structures were refined on F^2 by full-matrix least-squares methods using the *SHELXTL*–97 program package.[3] The solvate molecules of all data were treated as diffuse contribution to the overall scattering without specific atom positions by SQUEEZE/PLATON due to severe disorder of these solvate molecules in the lattices. The counter-anions in **3** could not be located due to serious disorder and weak diffraction. Several *t*Bu groups in clusters **2**–**4** and counter-anions in clusters **2** and **4** were located in statistic distribution due to disorder.

Computational Methodology. The calculations were implemented by using Gaussian 09 program package[4] for complexes **2**–**4**. The geometrical structures as isolated molecules in the ground state and the lowest-energy triplet state were firstly optimized, respectively, by the restricted and unrestricted density functional theory (DFT) method with the gradient corrected correlation functional PBE1PBE.[5] The initial structures were extracted from the experimentally crystallographic data. In order to rebuild the experimental absorption spectra, 80 singlet excited-states were calculated based on the optimized structures in the ground state to determine the vertical excitation energies by time-dependent density functional theory (TD-DFT)[6] with the same functional used in the optimization process. The single point energy calculations were performed based on the optimized lowest-energy triplet-state structures to obtain the orbital energy. In these calculations, the polarizable continuum model method (PCM)[7] using CH_2Cl_2 as the solvent was employed. The Stuttgart-Dresden (SDD)[8] basis sets and the effective core potentials (ECPs) were used to describe the Ag atoms, while other non-metal atoms of P, N, C and H were described by the all-electron basis set of 6-31G**.

References

[1] G. R. Newkome, D. C. Hager, *J. Org. Chem.* **1978**, *43*, 947–949.

[2] M. S. Bennington, H. L. C. Feltham, Z. J. Buxton, N. G. Whitea, S. Brooker, *Dalton Trans.* **2017**, *46*, 4696-4710.

[3] G. M. Sheldrick, *SHELXL-97, Program for the Refinement of Crystal Structures*; University of Göttingen: Göttingen, Germany, **1997**.

[4] M. J. Frisch, G. W. Trucks, H. B. Schlegel, G. E. Scuseria, M. A. Robb, J. R. Cheeseman, G. Scalmani, V. Barone, B. Mennucci, G. A. Petersson, H. Nakatsuji, M. Caricato, X. Li, H. P. Hratchian, A. F. Izmaylov, J. Bloino, G. Zheng, J. L. Sonnenberg, M. Hada, M. Ehara, K. Toyota, R. Fukuda, J. Hasegawa, M. Ishida, T. Nakajima, Y. Honda, O. Kitao, H. Nakai, T. Vreven, J. A. Montgomery, Jr., J. E. Peralta, F. Ogliaro, M. Bearpark, J. J. Heyd, E. Brothers, K. N. Kudin, V. N. Staroverov, T. Keith, R. Kobayashi, J. Normand, K. Raghavachari, A. Rendell, J. C. Burant, S. S. Iyengar, J. Tomasi, M. Cossi, N. Rega, J. M. Millam, M. Klene, J. E. Knox, J. B. Cross, V. Bakken, C. Adamo, J. Jaramillo, R. Gomperts, R. E. Stratmann, O. Yazyev, A. J. Austin, R. Cammi, C. Pomelli, J. W. Ochterski, R. L. Martin, K. Morokuma, V. G. Zakrzewski, G. A. Voth, P. Salvador, J. J. Dannenberg, S. Dapprich, A. D. Daniels, O. Farkas, J. B. Foresman, J. V. Ortiz, J. Cioslowski, D. J. Fox, *Gaussian 09, Revision D.01; Gaussian Inc.*, Wallingford, CT, 2013.

[5] J. P. Perdew, K. Burke, M. Ernzerhof, *Phys. Rev. Lett.* **1996**, *77*, 3865–3868.

[6] a) R. Bauernschmitt, R. Ahlrichs, *Chem*. *Phys*. *Lett*. **1996**, *256*, 454-464; b) M. E. Casida, C. Jamorski, K. C. Casida, D. R. Salahub, *J. Chem*. *Phys*. **1998**, *108*, 4439-4449; c) R. E. Stratmann, G. E. Scuseria, M. J. Frisch, *J. Chem*. *Phys*. **1998**, *109*, 8218-8224.

[7] a) V. Barone, M. Cossi, J. Tomasi, *J. Chem*. *Phys*. **1997**, *107*, 3210-3221; b) M. Cossi, G. Scalmani, N. Rega, V. Barone, *J. Chem*. *Phys*. **2002**, *117*, 43-54.

[8] D. Andrae, U. Häussermann, M. Dolg, H. Stoll, H. Preuss, *Theor. Chim. Acta* **1990**, *77*, 123-141.

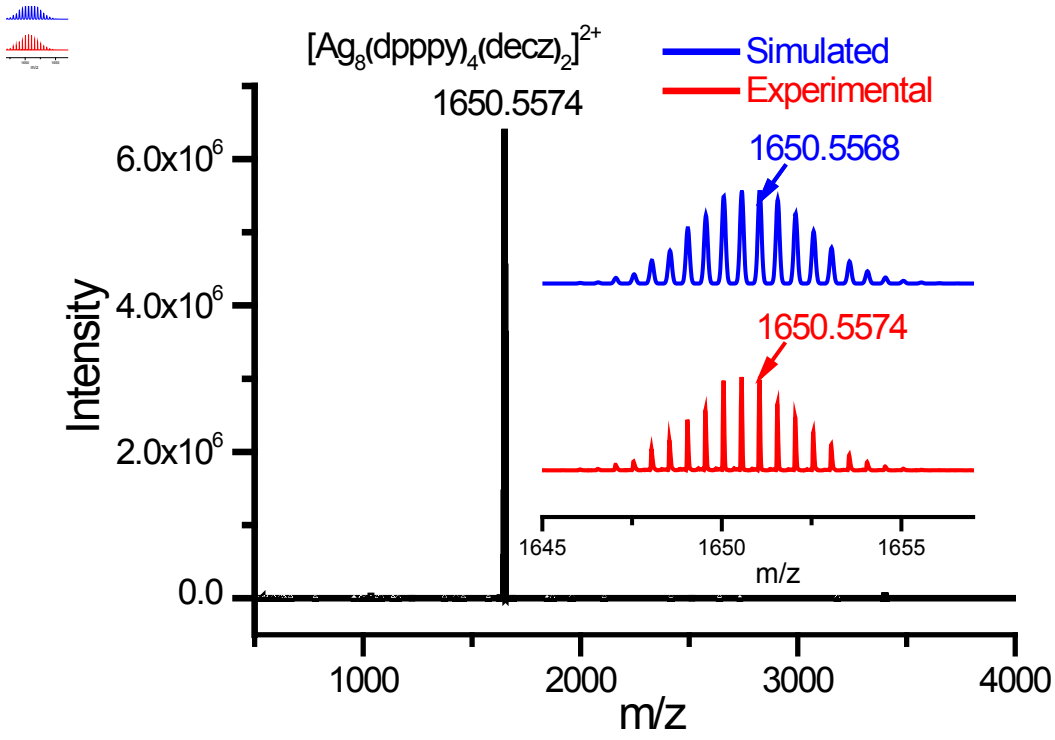

Figure S1. The HRMS of Ag_8 cluster complex **2**. Inset: The measured and simulated isotopic patterns.

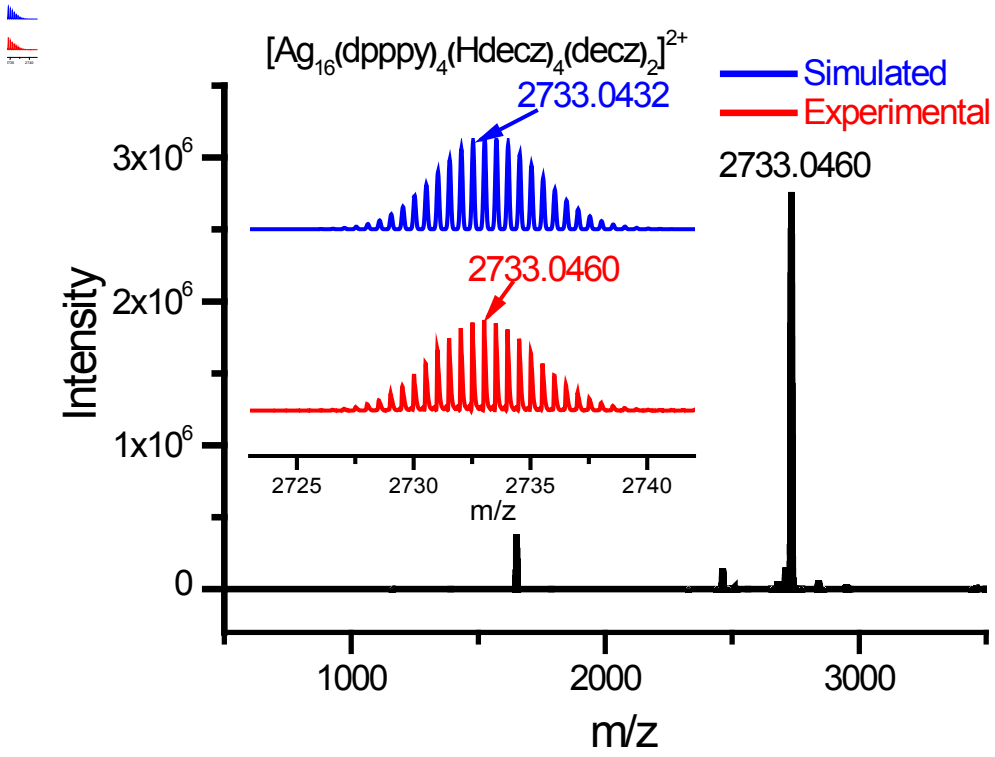

Figure S2. The HRMS of Ag_{16} cluster complex **3**. Inset: The measured and simulated isotopic patterns.

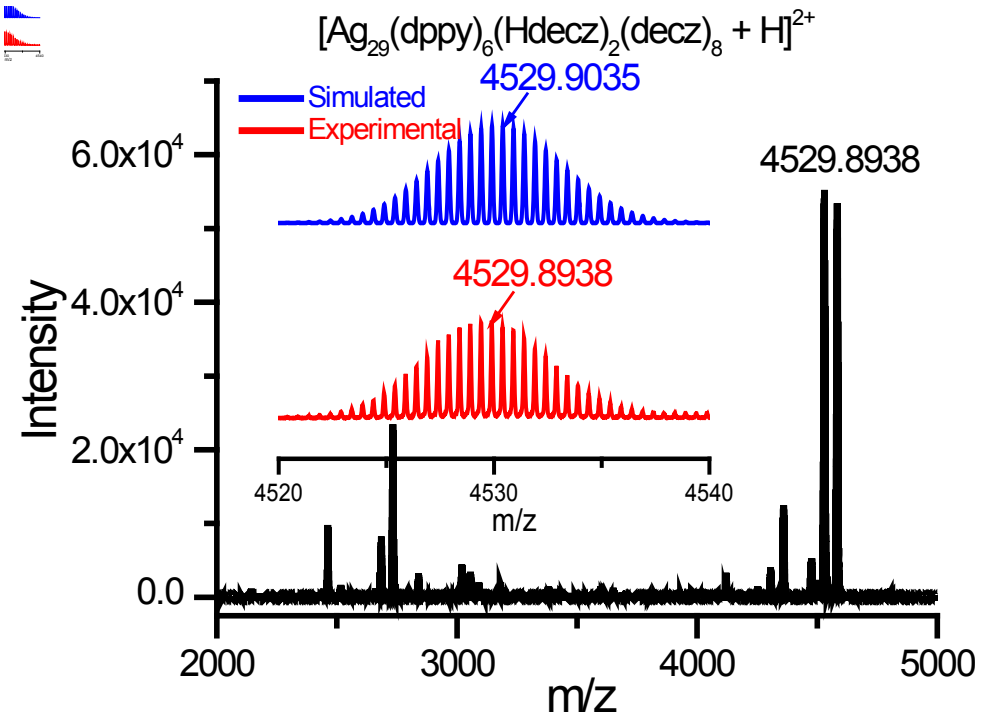

Figure S3. The HRMS of Ag_{29} complex **4**. Inset: The measured and simulated isotopic patterns.

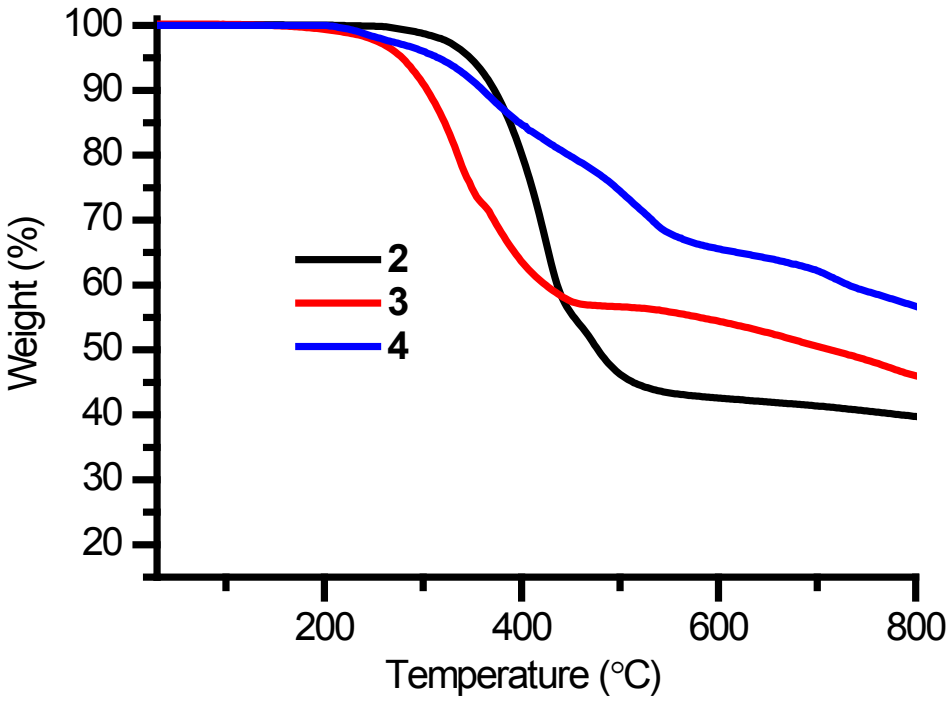

Figure S4. The polts of thermogravimetric analyses of cluster complexes **2**−**4**.

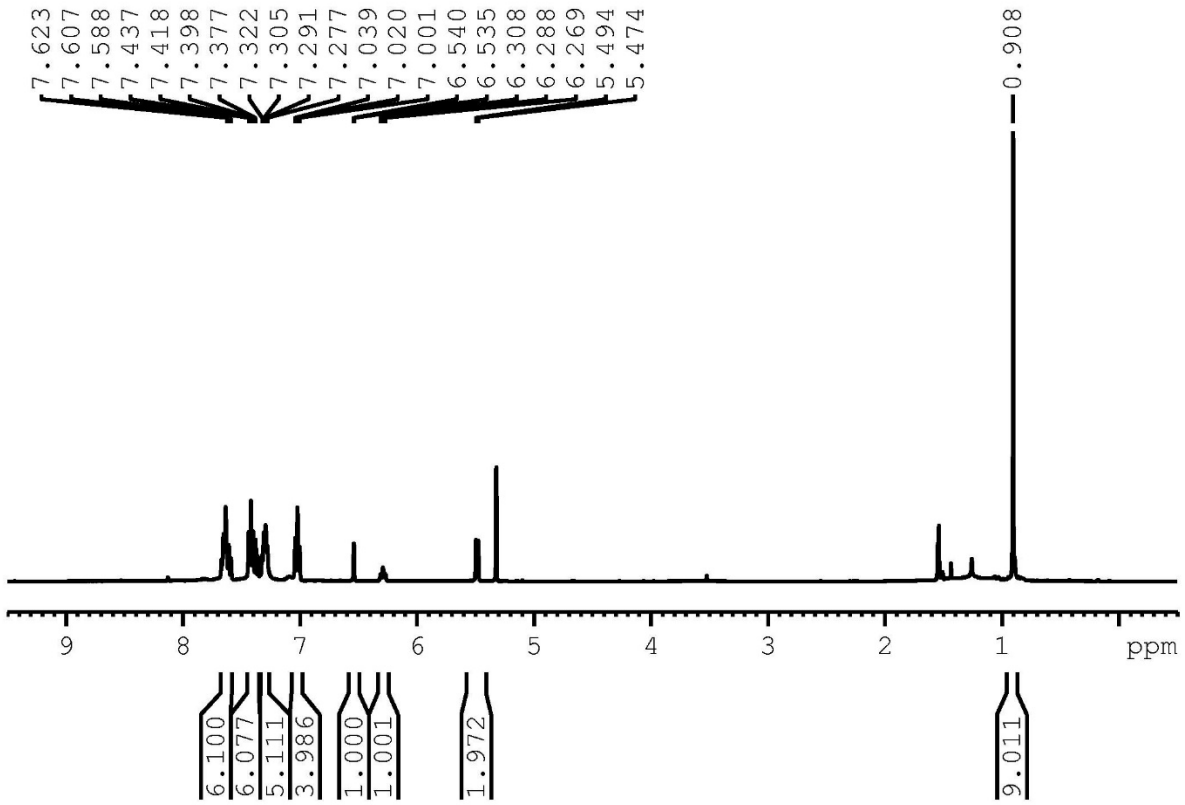

Figure S5. The ^{1}H NMR spectrum of Ag_8 complex **2** in CD_2Cl_2 solution at ambient temperature.

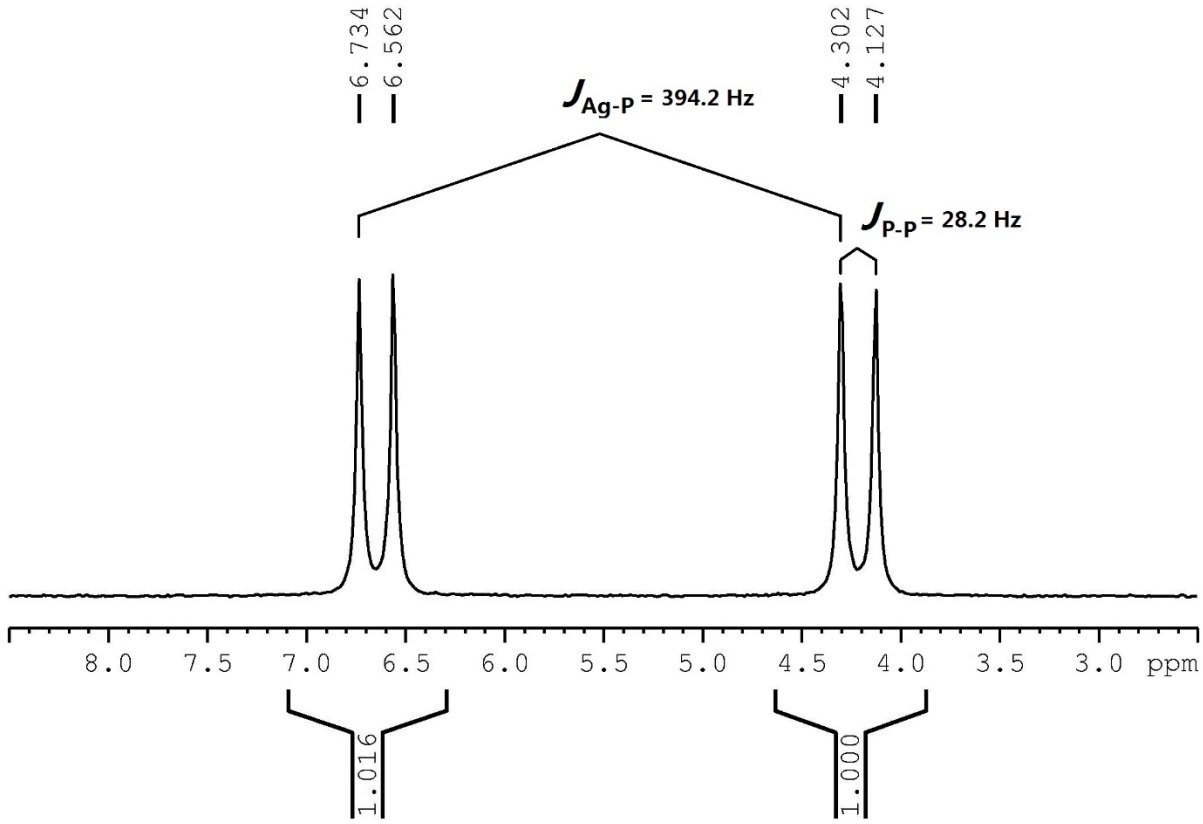

Figure S6. The ^{31}P NMR spectrum of Ag_8 complex **2** in CD_2Cl_2 solution at ambient temperature.

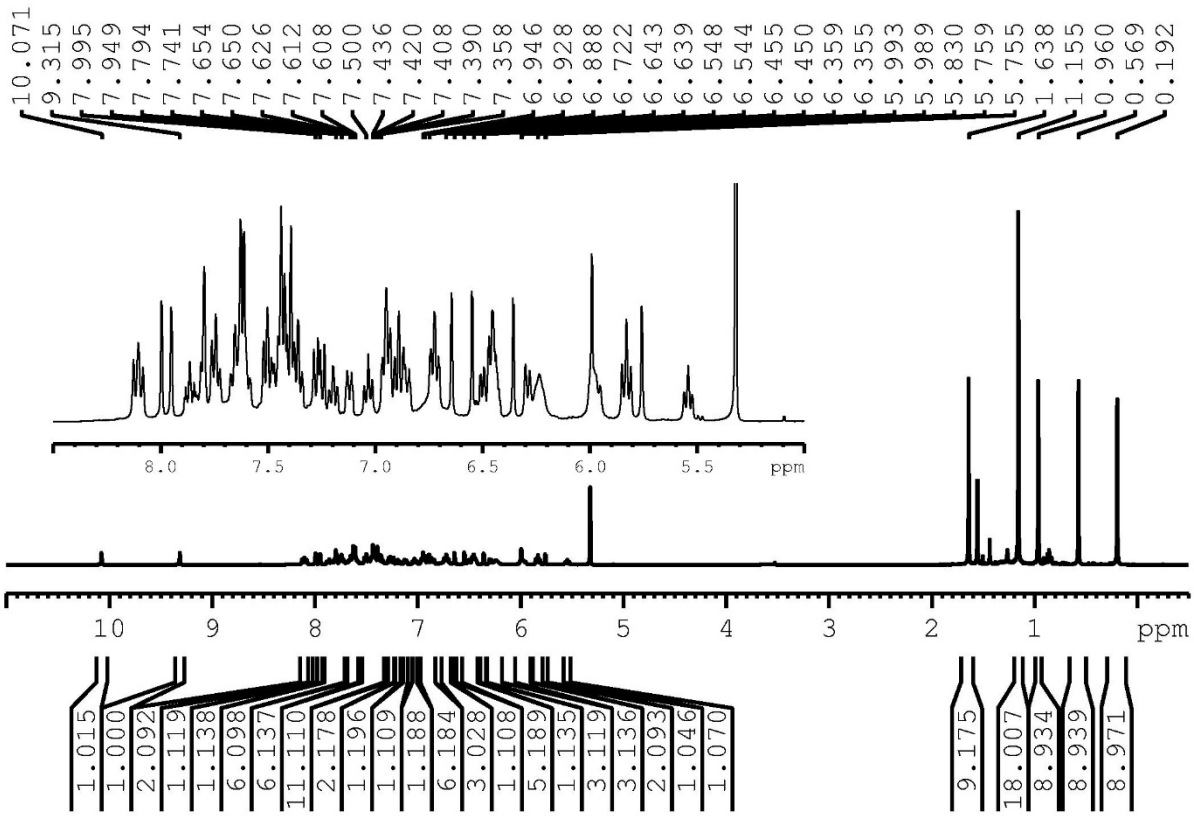

Figure S7. The ^{1}H NMR spectrum of Ag_{16} complex **3** in CD_2Cl_2 solution at ambient temperature.

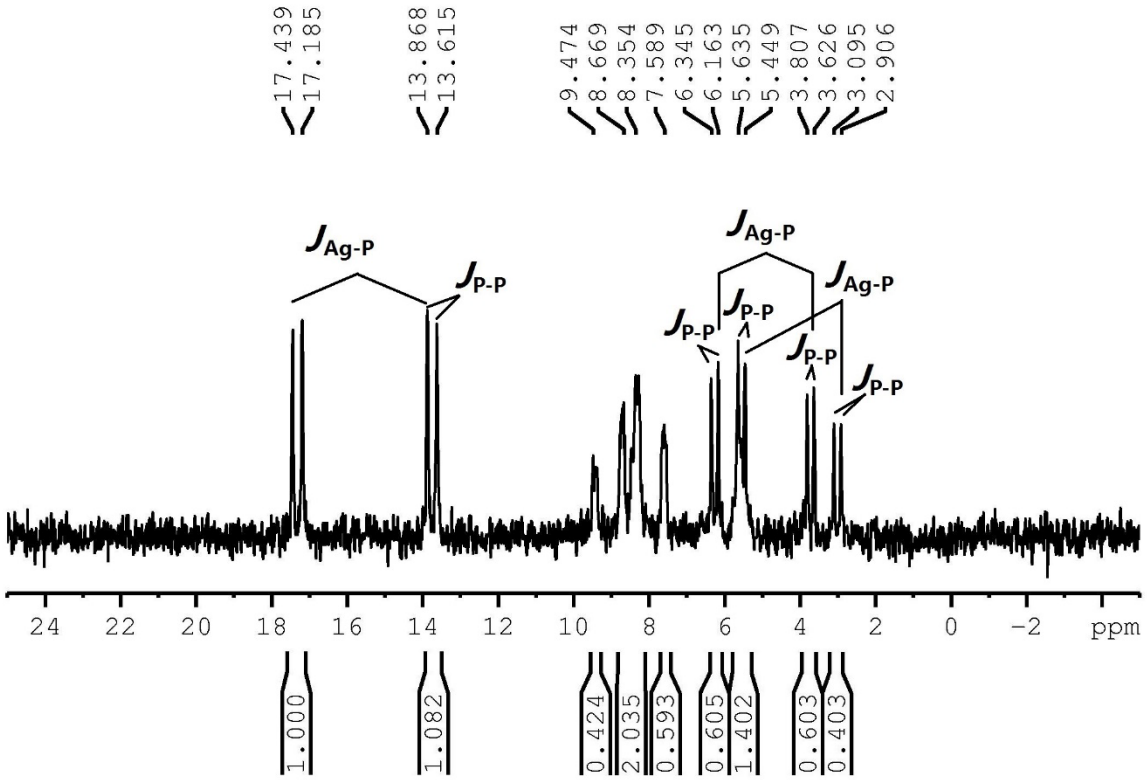

Figure S8. The ^{31}P NMR spectrum of Ag_{16} complex **3** in CD_2Cl_2 solution at ambient temperature.

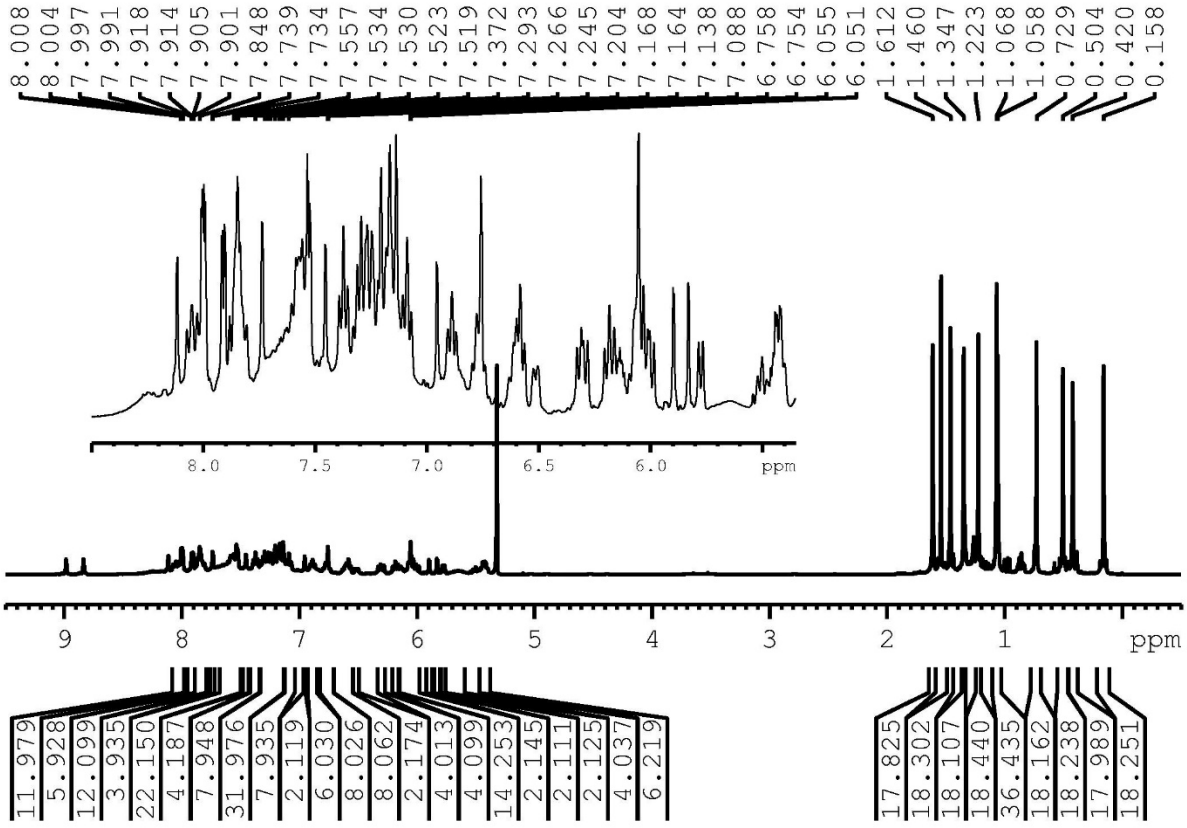

Figure S9. The ^{1}H NMR spectrum of Ag_{29} complex **4** in CD_2Cl_2 solution at ambient temperature.

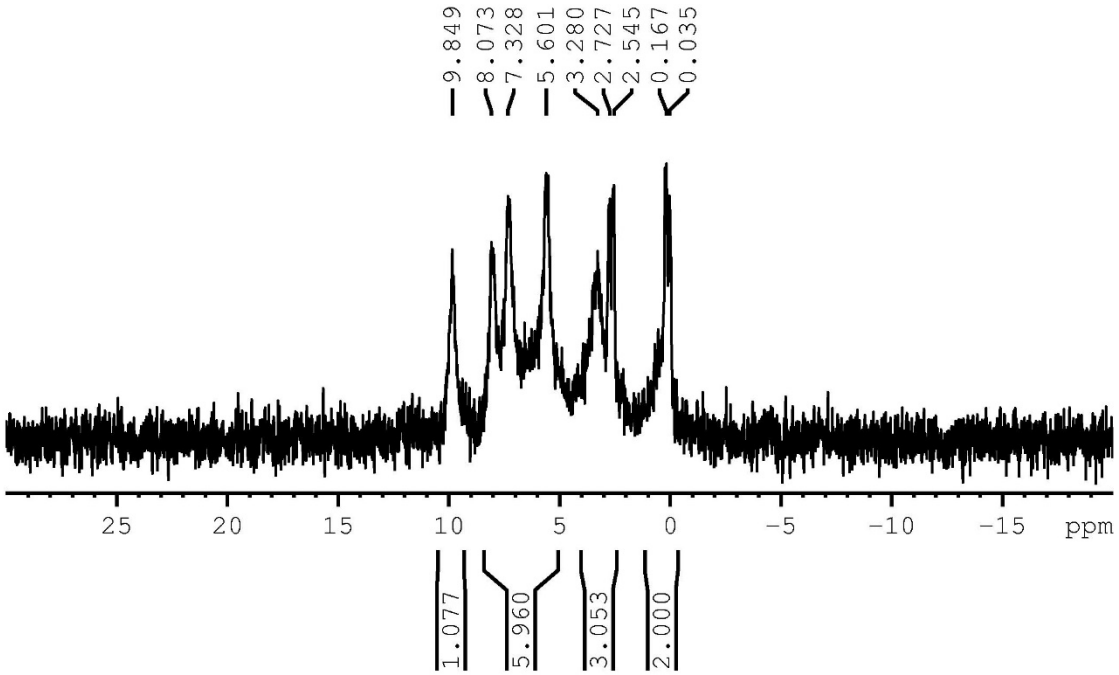

Figure S10. The ^{31}P NMR spectrum of Ag_{29} complex **4** in CD_2Cl_2 solution at ambient temperature.

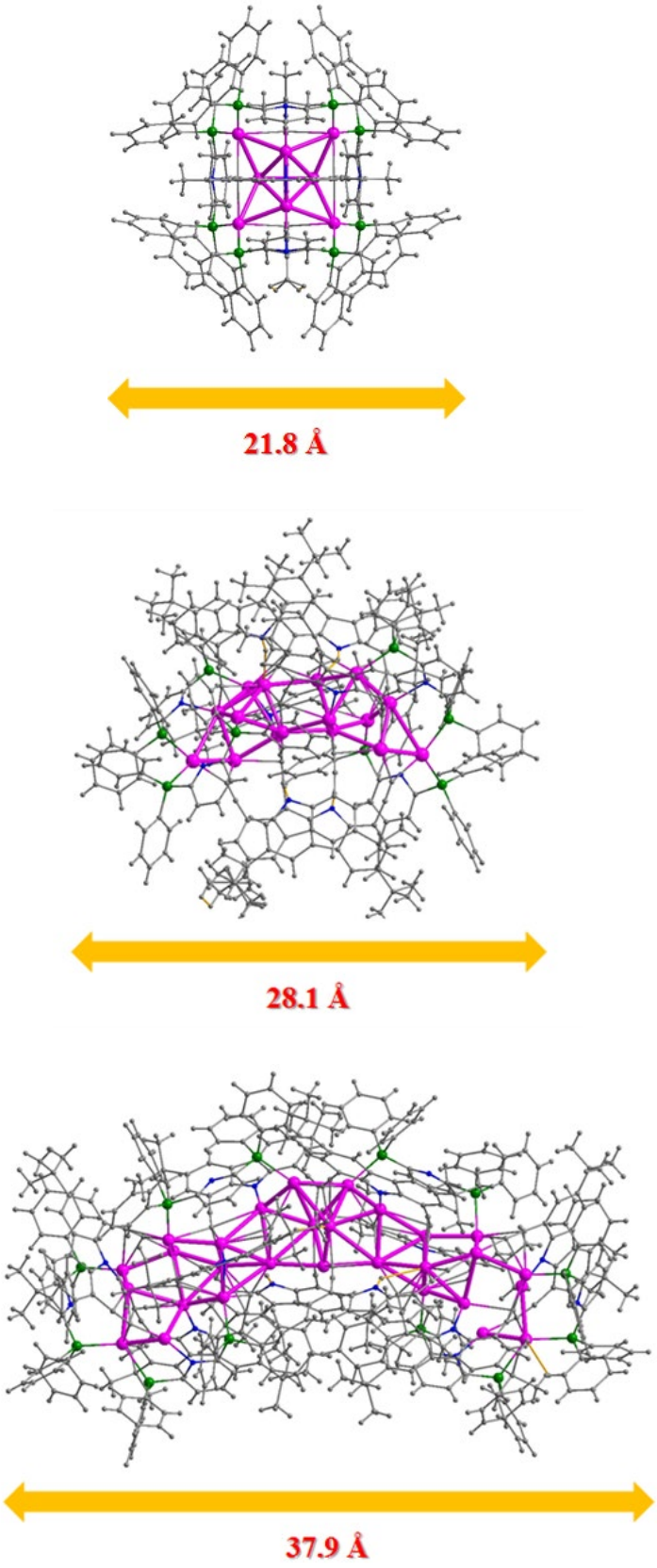

Figure S11. The molecular lengths of **2**−**4**.

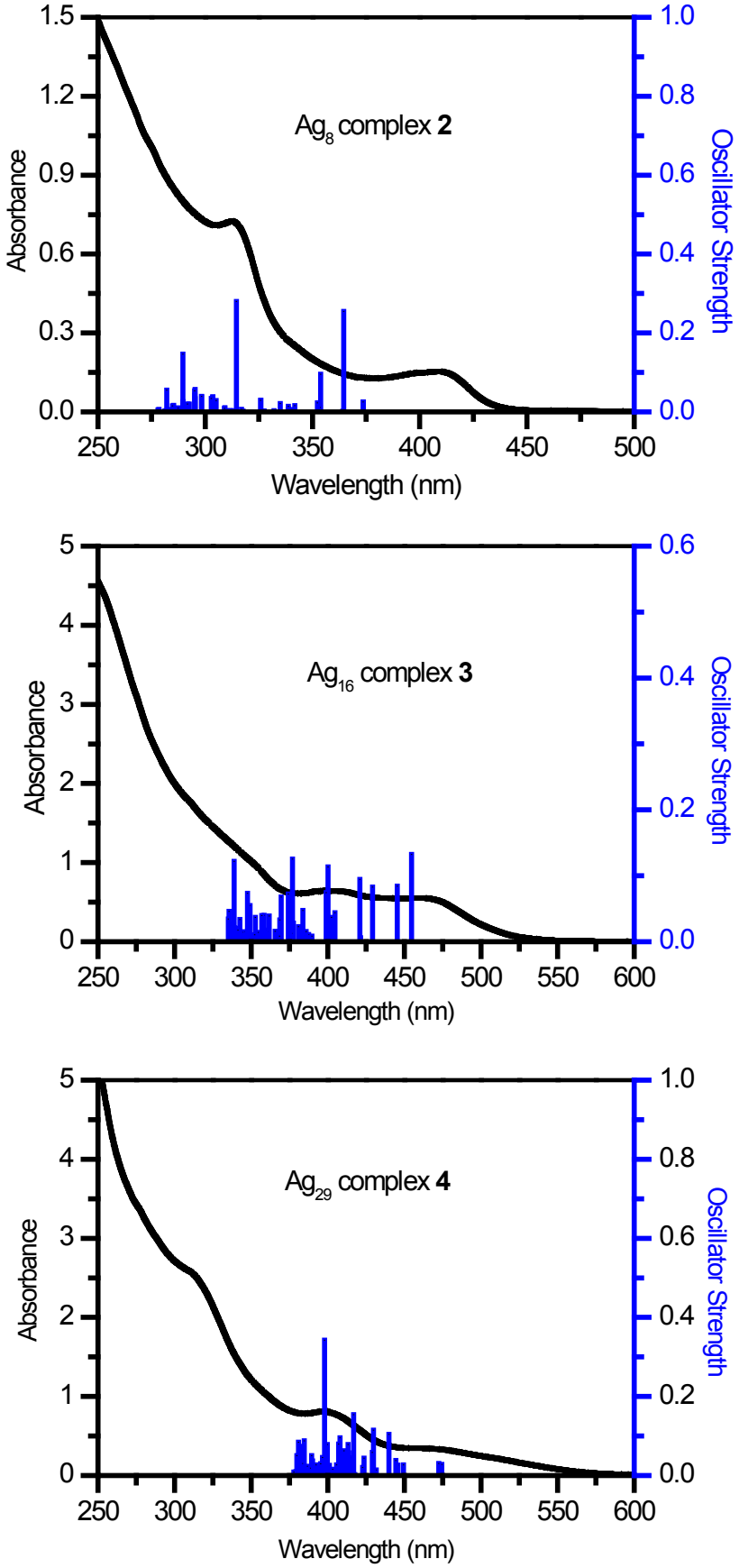

Figure S12. The calculated (blue vertical bars) and measured (black line) UV-Vis absorption spectra of complexes **2** (Ag_8), **3** (Ag_{16}) and **4** (Ag_{29}) in CH_2Cl_2 solution at ambient temperature by TD-DFT method at the PBE1PBE level.

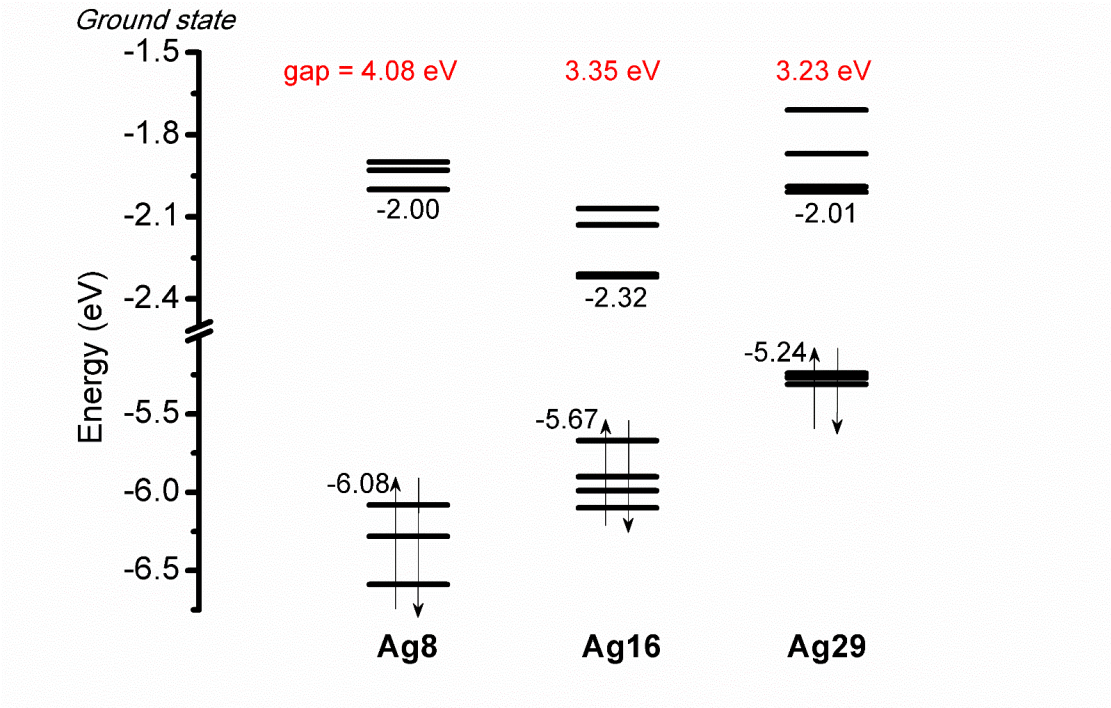

Figure S13. Plots of energy level of frontier orbitals (HOMO-3 to LUMO+3) for complexes **2** (Ag_8), **3** (Ag_{16}) and **4** (Ag_{29}) in the ground state in CH_2Cl_2 solution by TD-DFT method at the PBE1PBE level.

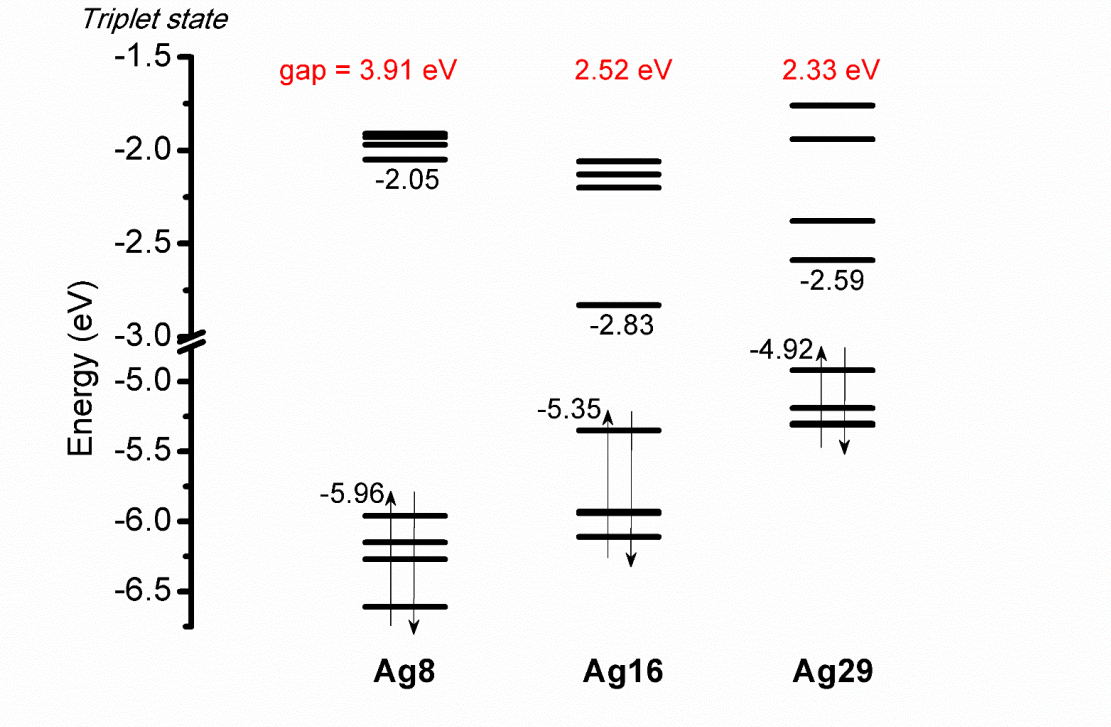

Figure S14. Plots of energy level of frontier orbitals (HOMO-3 to LUMO+3) for complexes **2** (Ag_8), **3** (Ag_{16}) and **4** (Ag_{29}) in the lowest-energy triplet state in CH_2Cl_2 solution by TD-DFT method at the PBE1PBE level.

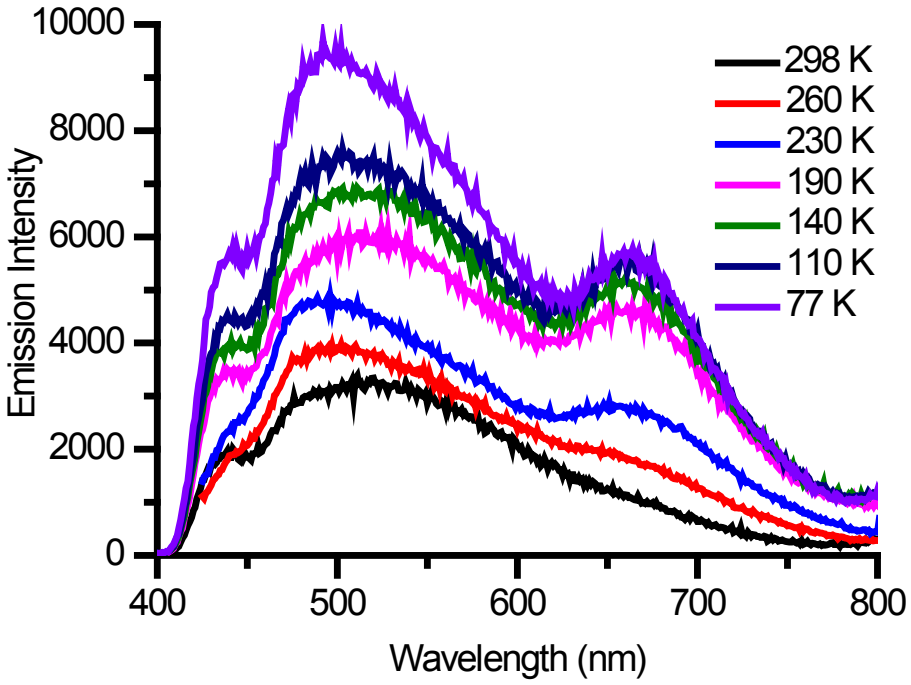

Figure S15. Temperature dependence of the emission spectra of **2** in solid state at 298–**77** K.

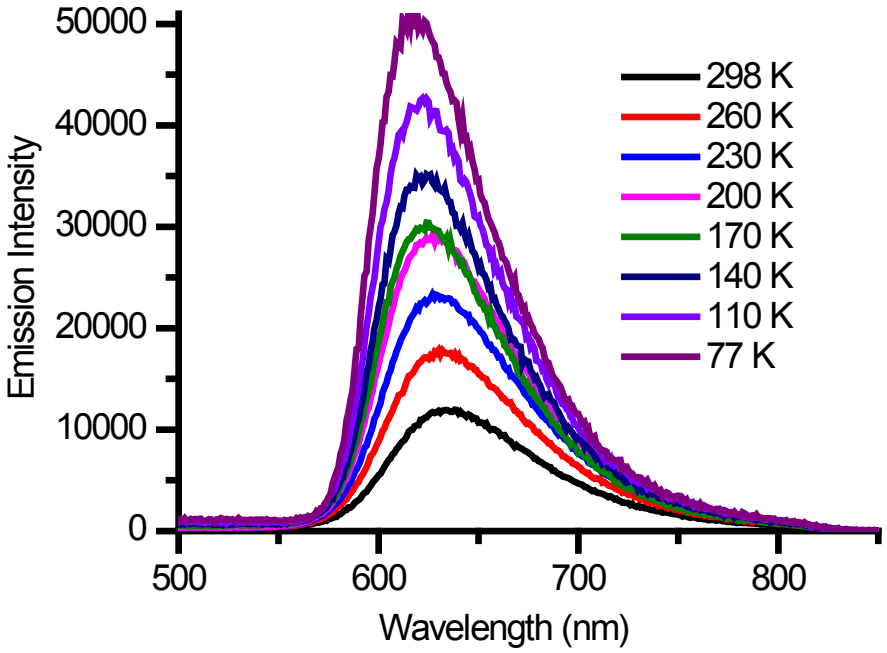

Figure S16. Temperature dependence of the emission spectra of **3** in solid state at 298–77 K.

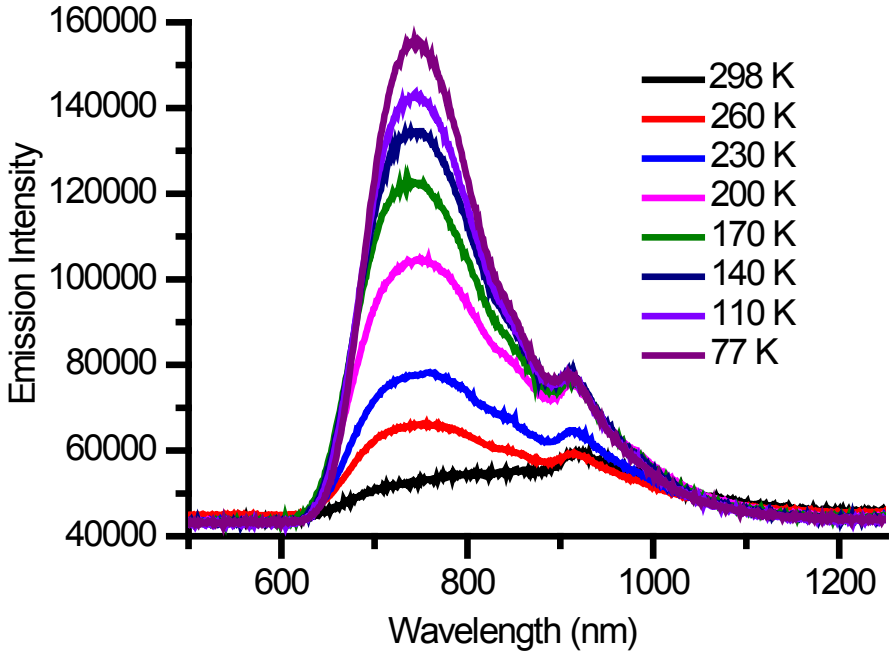

Figure S17. Temperature dependence of the emission spectra of **4** in solid state at 298–77 K.

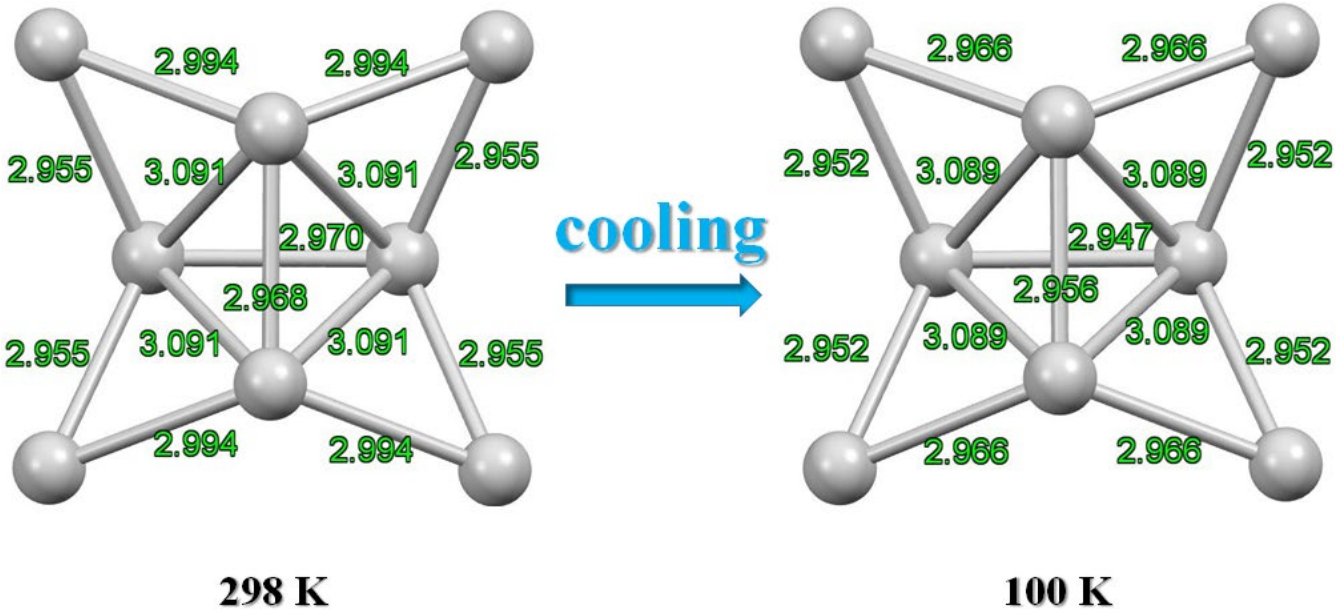

Figure S18. The Ag–Ag distances of Ag_8 cluster complex **2** at 298 (left) and 100 K (right).

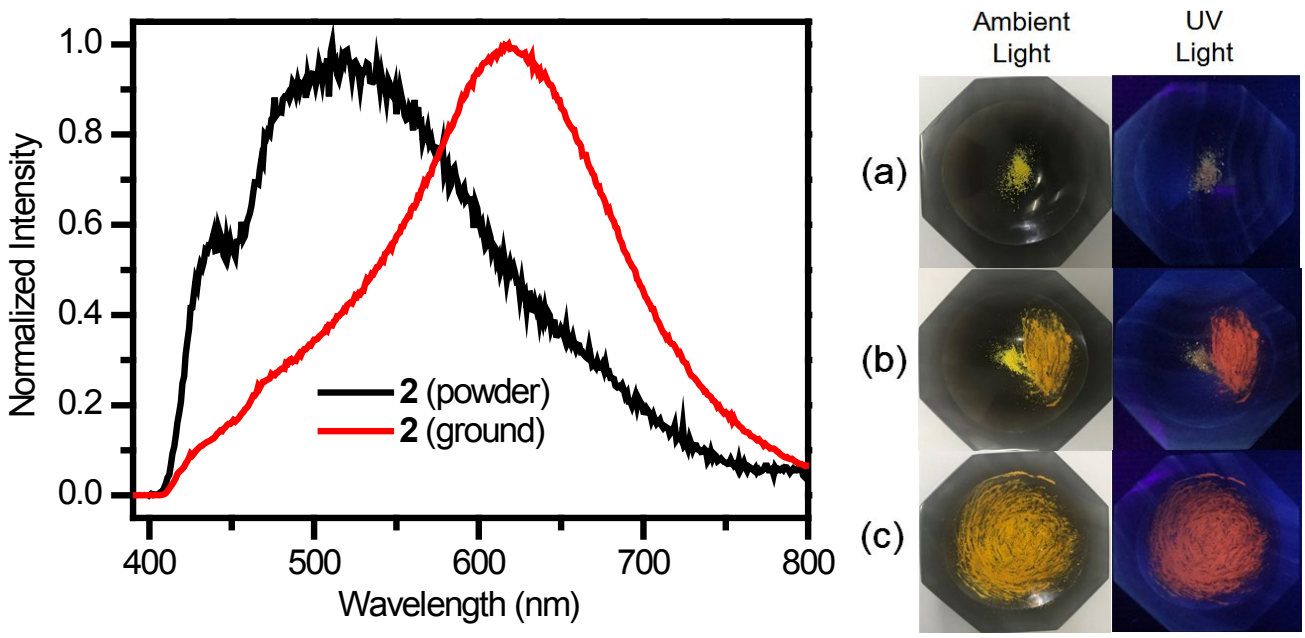

Figure S19. The normalized emission spectra of Ag_8 cluster complex **2** in crystalline and ground states (left). The photographic images of solid-state **2** in response to mechanical grinding under ambient light and UV light irradiation (365 nm). (a) Crystalline sample. (b) Partially ground sample. (c) Thoroughly ground sample.

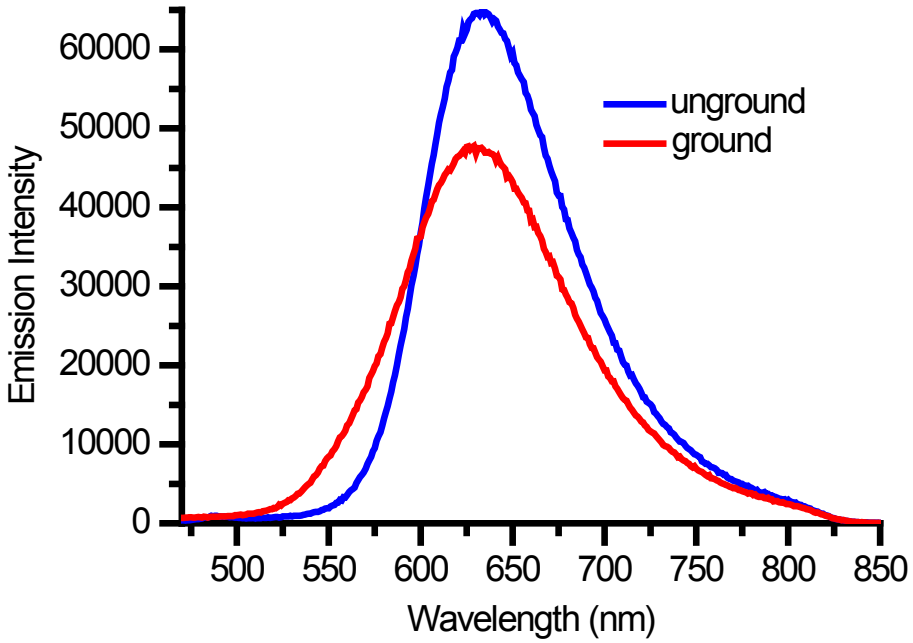

Figure S20. The emission spectra of Ag_{16} cluster complex **3** in crystalline and ground states.

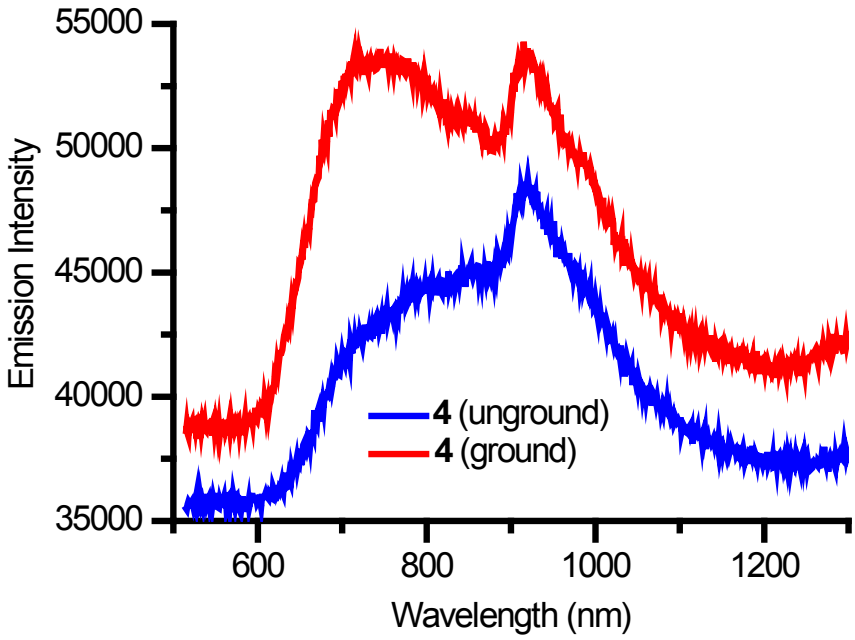

Figure S21. The emission spectra of Ag_{29} cluster complex **4** in crystalline and ground states.

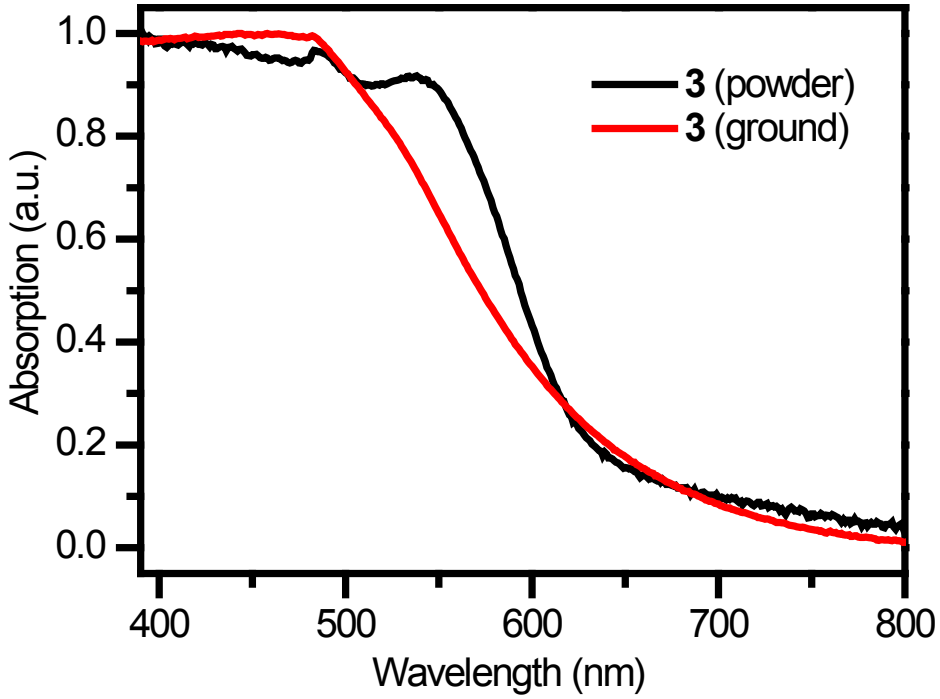

Figure S22. UV−Vis electronic spectra of Ag_{16} cluster complex **3** in crystalline and ground states.

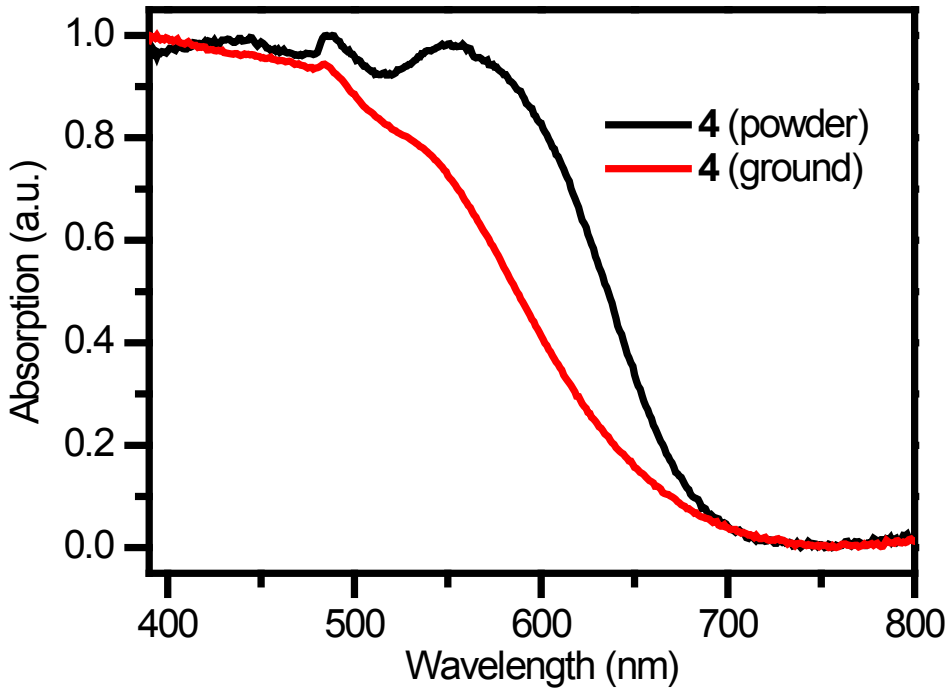

Figure S23. The UV−vis electronic spectra of Ag_{29} cluster complex **4** in crystalline and ground states.

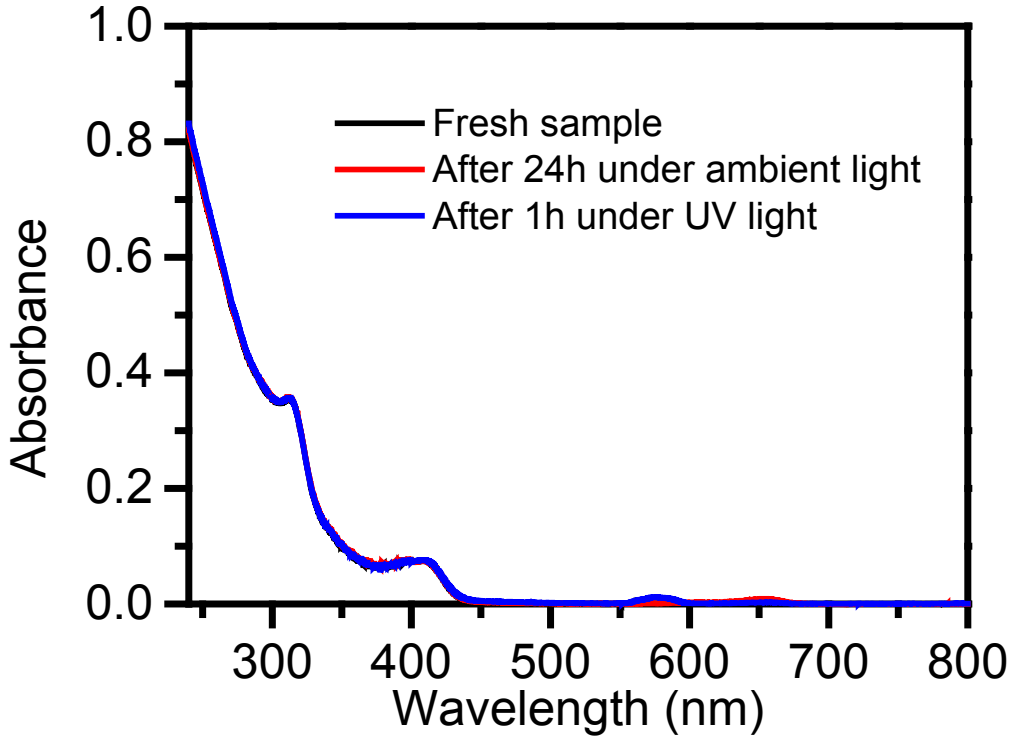

Figure S24. The stability check of **2** in CH_2Cl_2 solution by UV−vis spectra (0.5×10^{-5} mol/L).

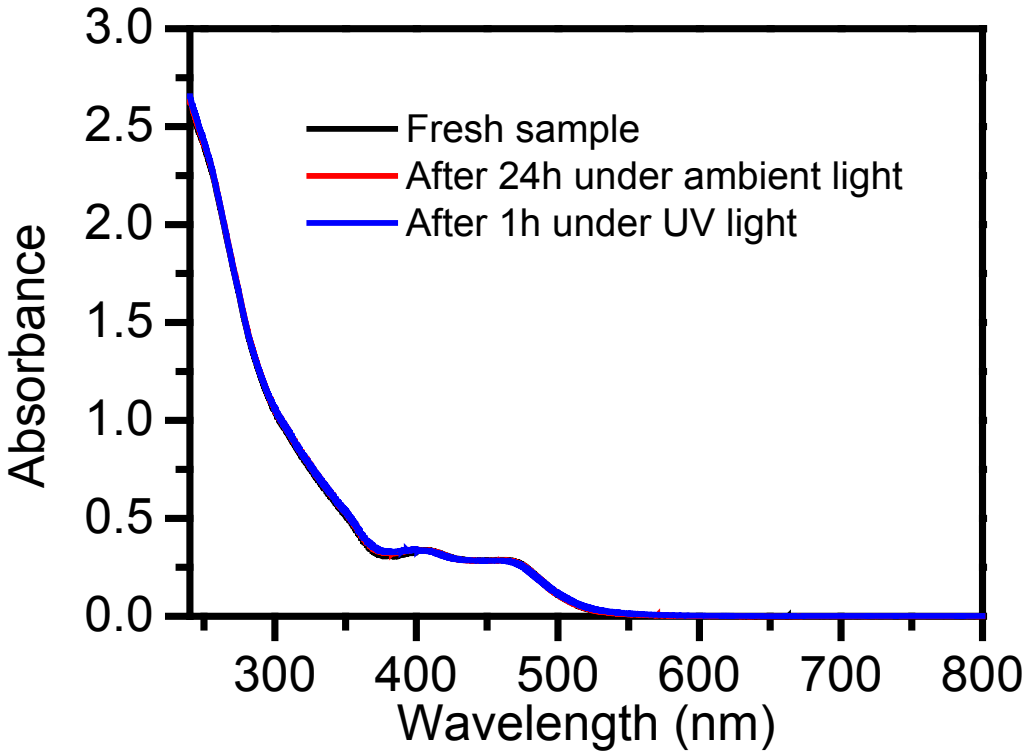

Figure S25. The stability check of **3** in CH_2Cl_2 solution by UV−vis spectra (0.5×10^{-5} mol/L).

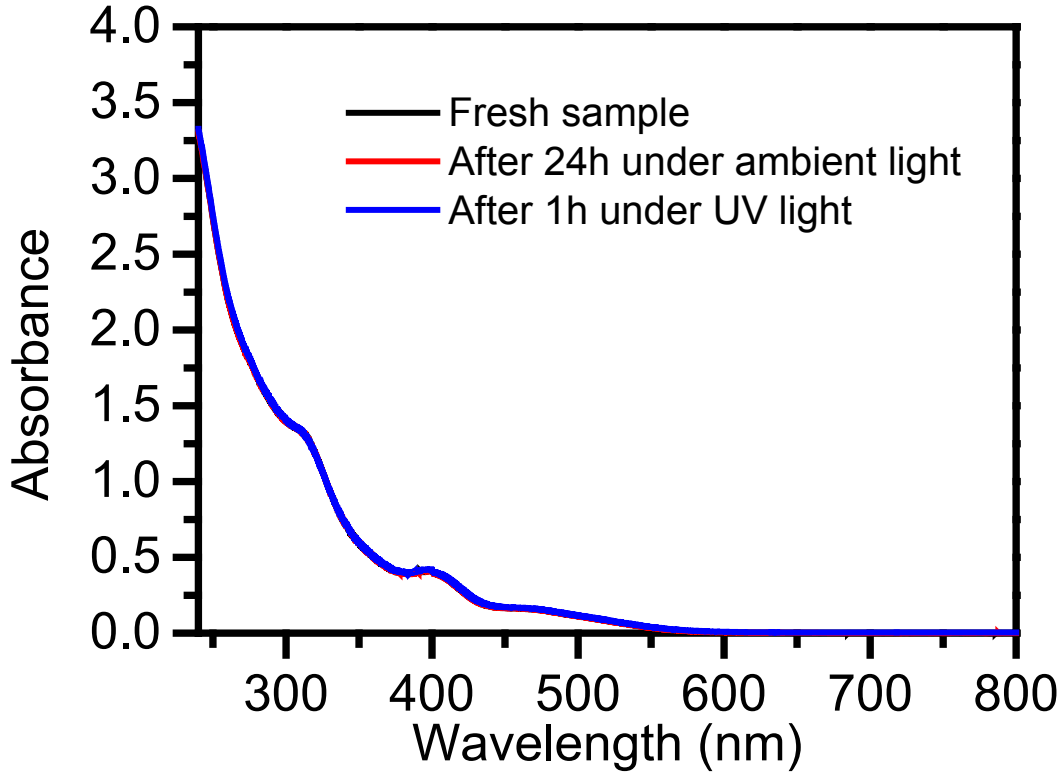

Figure S26. The stability check of **4** in CH_2Cl_2 solution by UV−vis spectra (0.5×10^{-5} mol/L).

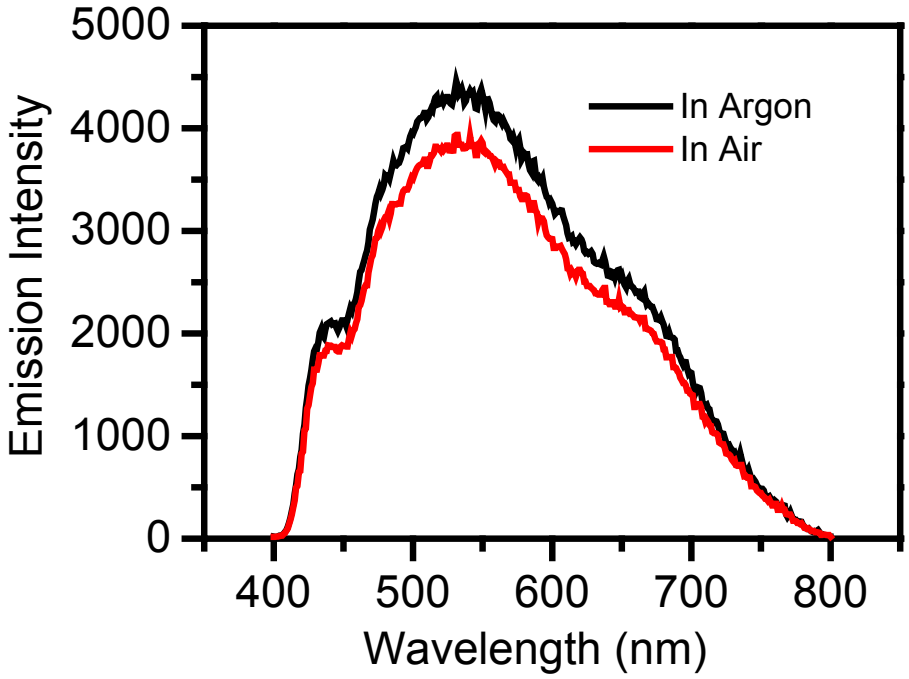

Figure S27. The emission spectra of fresh as-prepared sample **2** in argon and air.

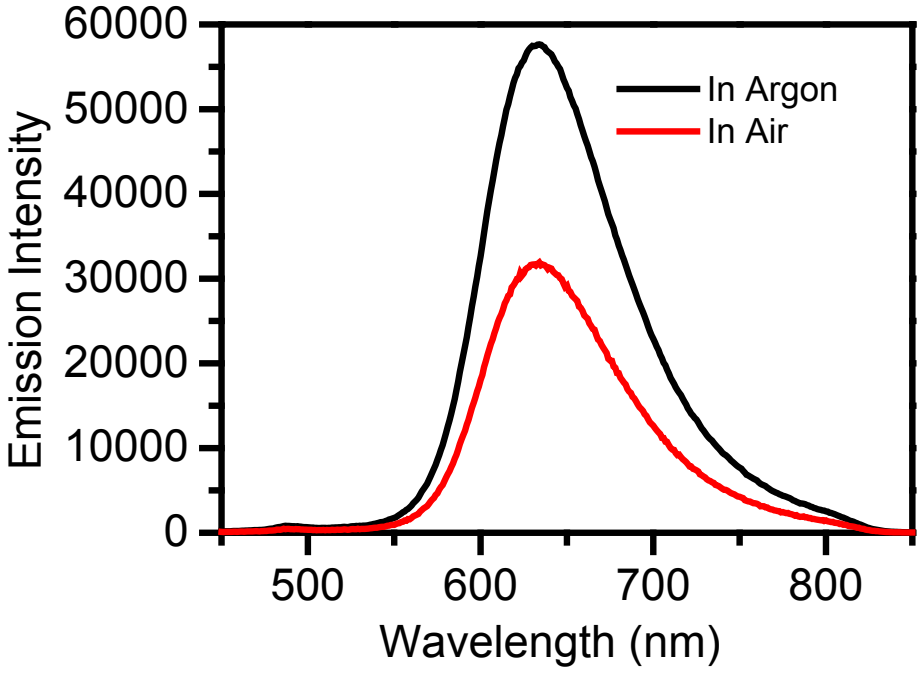

Figure S28. The emission spectra of fresh as-prepared sample **3** in argon and air.

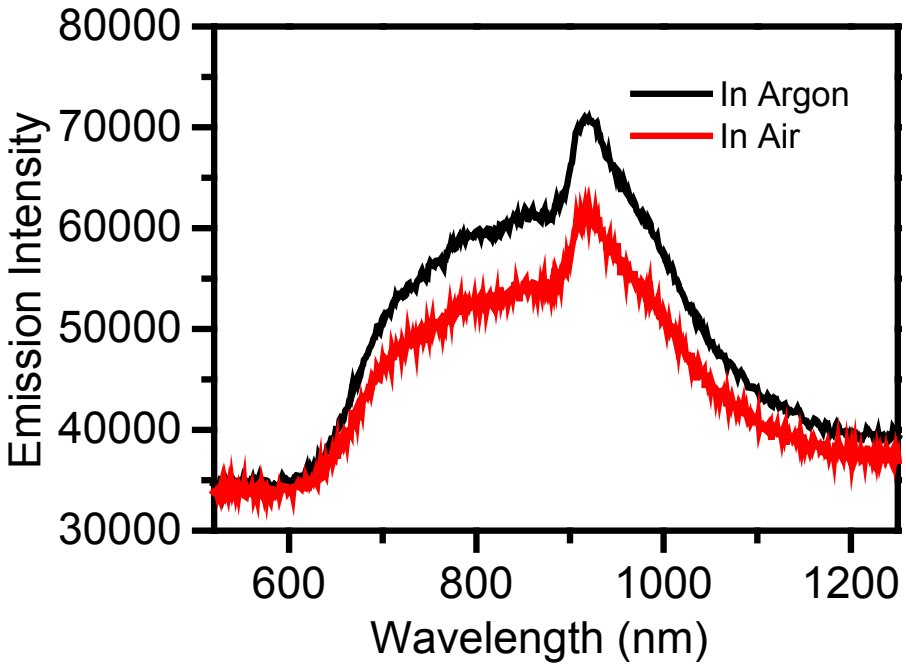

Figure S29. The emission spectra of fresh as-prepared sample **4** in argon and air.

Table S1. The UV-Vis Absorption Spectral Data of Complexes **2**–**4** in CH_2Cl_2 at Ambient Temperature.

	λ_{abs}/nm (ε/dm^3 mol^{-1} cm^{-1})
2	253 (142030), 313 (72350), 409 (15240)
3	251 (449000), 310 (176350), 402 (64230), 463 (54880)
4	243 (615670), 311 (257030), 398 (82250), 470 (34440), 510 (21730)

Table S2. Crystallographic data of complexes **2**–**4**.

compound (temp.)	**2** (298 K)	**2** (100 K)	**3** (100 K)	**4** (100 K)
empirical formula	$C_{164}H_{136}Ag_8Cl_2N_6O_8P_8$	$C_{164}H_{136}Ag_8Cl_2N_6O_8P_8$	$C_{260}H_{228}Ag_{16}Cl_2N_{10}O_8P_8$	$C_{414}H_{360}Ag_{29}ClN_{16}O_4P_{12}$
formula weight	3500.40	3500.40	5665.09	9158.48
crystal system	orthorhombic	orthorhombic	triclinic	triclinic
space group	*Cmcm*	*Cmcm*	$P\bar{1}$	$P\bar{1}$
a (Å)	23.3532(8)	23.0100(16)	20.418(4)	22.522(5)
b (Å)	27.1392(8)	26.8097(16)	32.912(7)	27.590(6)
c (Å)	25.6913(8)	24.9769(16)	44.298(9)	37.588(8)
α (deg)	90	90	104.94(3)	69.16(3)
β (deg)	90	90	90.19(3)	78.44(3)
γ (deg)	90	90	94.68(3)	84.54(3)
V (Å^3)	16282.8(9)	15408.1(17)	28656(11)	21379(9)
Z	4	4	4	2
ρ_{calcd} (g/cm^{-3})	1.428	1.509	1.313	1.423
μ (mm^{-1})	1.107	1.170	1.178	1.394
radiation (λ, Å)	0.71073	0.71073	0.82634	0.62285
temperature (K)	298(2)	100(2)	100(2)	100(2)
GOF	0.950	1.096	1.015	1.049
R1 (F_o)[a]	0.0462	0.0989	0.1155	0.0747
*w*R2 (F_o^2)[b]	0.2011	0.2612	0.3225	0.2336

[a] $R1 = \Sigma|F_o - F_c|/\Sigma F_o$, [b] $wR2 = \Sigma[w(F_o^2 - F_c^2)^2]/\Sigma[w(F_o)^2)]^{1/2}$